Polym. Bull. (2010) 64:375–386
DOI 10.1007/s00289-009-0188-y

ORIGINAL PAPER

Preparation and characterization of crosslinked poly(methylmethacrylate) heat sensitive color-developing nanocapsules

Puying An · Xinwu Ba · Shuang Lu

Received: 2 May 2009 / Revised: 6 October 2009 / Accepted: 7 October 2009 /
Published online: 18 October 2009

Abstract The crosslinked poly(methylmethacrylate) (PMMA) heat sensitive color-developing nanocapsules were prepared by emulsion polymerization, in which leucocompound was used as a core material and methyl methacrylate and unsaturated hyperbranched poly(amide-ester) as wall-forming materials. The nanocapsules were characterized by Malvern particle size analysis, scanning electron microscopy, Fourier transform infrared spectrophotometry (FTIR), thermo-gravimetric analysis (TGA), differential scanning calorimetry (DSC), and densitometry. Triton X-100 was used as the emulsifier of emulsion polymerization. The effects of the emulsifier content on the particle size distribution and morphology of nanocapsules were discussed in detail. The FTIR analysis of leucocompound-containing nanocapsules demonstrated that leucocompound was successfully encapsulated in the crosslinked PMMA matrix. TGA results showed that the resultant nanocapsules had good thermal stabilities. The DSC analysis of the resultant nanocapsules indicated that the glass transition temperature of the nanocapsules was 117.9 °C. The resultant nanocapsules had narrower particle size distribution, smoother surface, and higher heat sensitive color-developing density with the percentage weight of emulsifier being 0.6 wt%.

Keywords Heat sensitive color-developing nanocapsules · Emulsion polymerization · Crosslinked poly(methylmethacrylate) · Leucocompound

P. An (✉) · X. Ba · S. Lu
College of Chemistry and Environmental Science, Hebei University, Baoding 071002, Hebei, People's Republic of China
e-mail: anpuying@yahoo.com.cn

Introduction

Heat sensitive color-developing nanocapsules encapsulating a leucocompound have been widely employed in the heat-sensitive recording material such as medicinal images, facsimiles, printers, labels [1], etc. The leucocompound is an electron-donating dye precursor, which reacts with the electron-accepting compound (developer) to develop a color. However, because of very strong activity of leucocompound it is hoped to coat leucocompound with a protective matrix or wall of synthetic or natural polymers by nanoencapsulation technique [2]. In other words, the sensitive leucocompound is first isolated from the external medium in order to avoid the adverse reaction at ambient temperature. And then when the wall of the nanocapsule is heated above its glass transition temperature, the material transmittance of the wall increases and the leucocompound contained in the core of the nanocapsule and the developer outside of the nanocapsule transmits the wall of the nanocapsule to develop a color, in which the nanocapsule is not broken by heat and has the heat-sensibility control ability [1, 3–5].

Among many nanoencapsulation approaches, the emulsion polymerization is one of the most feasible methods [6, 7]. The key for the nanocapsule preparation by emulsion polymerization is that the organic phase containing a core material is dispersed into fine droplets. And then polymerization is initiated on the surface of core material to form nanocapsules. Hence it is essential to select the adequate emulsifier [8]. And MMA is a monomer which is in common used by emulsion polymerization. PMMA is a thermoplastic resin with excellent physical and chemical properties such as abrasion resistance, water repellency, high degree of transparency, etc., and wide applications containing adhesives, paints, drugs. and so on [9]. Moreover, the attention to hyperbranched polymers (HBP) is rapidly growing due to their unique physical and chemical properties such as low viscosity, high solubility, and possessing high density of functional terminal groups to be accessible for chemical modification [10–12]. Therefore, HBPs are attractive for some applications such as adhesive, cross-linking agents, and viscosity modifiers [13, 14]. As a result, crosslinked PMMA with unsaturated hyperbranched poly(amide-ester) (UHBP) as cross-linking agent has many advantages such as non-toxicity, high degree of transparency, compact property.

In this study, heat sensitive color-developing nanocapsules with the crosslinked poly(methyl methacrylate) (PMMA) as wall-forming material was prepared by emulsion polymerization, in which unsaturated hyperbranched poly(amide-ester) was used as the cross-linking agent and Triton X-100 was used as the emulsifier. The effects of the emulsifier content on the particle size distribution and morphology of nanocapsules were discussed in detail. The aim of the study is to gain a better understanding of the fundamentals of crosslinked PMMA with unsaturated hyperbranched poly(amide-ester) as the cross-linking agent applied to preparation of heat sensitive color-developing nanocapsules, which lays the foundation for further studies of crosslinked PMMA nanocapsule such as its application to the heat-sensitive recording material.

Experimental

Materials

Methyl methacrylate (MMA, distilled under vacuum prior to use) purchased from Tianjin Huadong Reagent Factory was used as a wall-forming material. Ammonium persulfate (APS) purchased from Beijing the Third Chemical Reagent Factory was used as an initiator. Triton X-100 purchased from Shanghai Tianlian Fine Chemical Reagent Co. was used as an emulsifier. Poly(vinyl alcohol) 224 (PVA 224) purchased from Junsei Chemical was used as the protective colloid [15]. Ethyl acetoacetate obtained from Tianjing Damao Chemical Reagent Factory and ethyl acetate obtained from Tianjin Meilin Chemical Co. were used as the high and low boiling point solvents for the leucocompound, respectively. The leucocompound used as a core material was 2-Phenylamino-3-methyl-6-(di-*n*-butylamino)fluorane and was obtained from Jiangsu Longsheng Co. Benzyl *p*-hydroxybenzoate obtained from Jiangsu Longsheng Co. was used as a developer. All the purchased reagents were in analytical grade. Hyperbranched unsaturated poly(amide-ester) (UHBP) ($\bar{M}_w$, 3,775) produced according to the literature was used as the cross-linking agent [16].

Preparation of nanocapsules

In a typical synthesis, 1.2 g of the leucocompound was previously dissolved in 1.2 g of ethyl acetoacetate and 5.6 g of ethyl acetate. The prepared solution that became an oil component in the system was poured into 32.0 g of aqueous solutions containing 1.8 g of PVA224 and the desired amount of Triton X-100 (see Table 1). The mixture was then vigorously agitated at 6,500 r/min for 12 min with a homogenizer (BME100L, Shanghai Weiyu Co.) to obtain o/w emulsion. The o/w emulsion was poured into a four-necked flask equipped with a magnetic stirrer (Tokyo Rikakikai Co., Ltd.), a thermometer, and a nitrogen gas inlet and outlet. Then the flask was immersed into a 70 °C oil bath and the nitrogen gas was bubbled through the solution for deoxygenation. The stirring speed was fixed at 500 r/min. After 20 min, 9.6 g of freshly distilled MMA and 0.6 g of the cross-linking agent (UHBP) was poured into the reaction flask and stirred for 15 min. Then 0.06 g APS was added into the reactor. The polymerization was carried out at 70 °C for 5 h. The obtained nanocapsule slurry was first washed with distilled water and recentrifuged three times at 16,000 r/min for 20 min, and then washed with ethyl acetate to

Table 1 Recipes of aqueous phase for the o/w emulsion preparation

Sample no.	PVA (g)	Percentage weight of emulsifier[a] (wt%)	Aqueous phase (g)
1	1.8	0.1	32.0
2	1.8	0.3	32.0
3	1.8	0.6	32.0
4	1.8	0.9	32.0

o/w emulsion: 40.0 g

[a] Based on o/w emulsion

remove free leucocompound on their surfaces and dried for at least 24 h under reduced pressure at ambient temperature.

Characterizations of nanocapsules

The average hydrodynamic diameter (d) and size distribution were measured by zeta potential and particle size analyzer (Zetasizer 3000HS, Malvern Instruments, UK). Before measurement, the samples were diluted with deionized water at 1:5,000 volume ratio. The morphology of the nanocapsules was observed by scanning electron microscopy (SEM, JSM-5400, JEOL, Japan). The nanocapsules were sprinkled onto a double-sided tape, sputter-coated with gold, and examined in the microscope using the accelerated voltage of 30 kV. The IR spectra were recorded with a Fourier transform infrared spectrophotometer (Vector22, Bruker Co., Germany). The sample were ground with dried KBr powder, and compressed into a plate. The KBr plate was scanned by a FTIR spectrophotometer. The thermo-gravimetric analysis was determined by thermo-gravimetric analysis (TGA, Perkin Elmer Co., USA). About 5 mg of sample was put into a crucible for thermo-gravimetric analysis. The heating rate was 20 °C/min in a stream of nitrogen with a flow rate of 20 mL/min. The recorded temperature range was from 50 to 850 °C. The glass transition temperatures (T_g) of dried samples were investigated by differential scanning calorimetry (Diamond DSC, Perkin Elmer Co., USA). Each sample of about 5 mg was primarily heated from 25 to 160 °C at 20 °C/min heating rate and then were cooled to 25 °C. Second, the samples were reheated to 160 °C. The T_g of the sample was determined from the second cycle where the highest point of the inflection was taken as the T_g. All operations were carried out in a stream of nitrogen with a flow rate of 20 mL/min.

Determination of nanocapsule encapsulation efficiency

The encapsulation efficiency of the resultant nanocapsules was determined by extraction with ethyl acetoacetate. First, the nanocapsule samples were ground with a mortar and pestle at room temperature. The dried and ground nanocapsule was weighed (W_1) and was sealed in a filter paper bag. Then, the sample bag was placed in a Soxhlet apparatus, extracted with ethyl acetoacetate for 12 h, and dried in a vacuum oven at 60 °C. After cooling in a vacuum desiccator, the sample bag was weighed again (W_2). Eventually, the encapsulation efficiency of the nanocapsules was calculated by:

$$\phi(\text{wt\% }) = \frac{W_1 - W_2}{W_0} \times 100 \tag{1}$$

where W_0 denotes the weight of leucocompound in feed.

Heat sensitive color-developing properties

The heat sensitive color-developing property measurement was performed by a conventional method [17]. The mixture containing 1.0 g of nanocapsule and 0.5 g

of developer suspension was dipped on a polyethylene terephthalate (PET) film, spread homogeneously with a wire bar, and dried completely by a dryer. The protective colloid, PVA, played the role of a binder between the PET sheet and the nanocapsule thin layer. The thickness of the coating layer was ca. 15 μm, which was evaluated by a thickness analyzer (Carl Zeiss Jena Co., Germany). The color yield of color-produced nanocapsules was evaluated as the transmission density. And then the transmission density by using a thermal printer with changing heat energy applied to a thermal head was measured using an X-Rite-310 densitometer (Michigan Co., USA).

Results and discussion

Effects of the emulsifier content on the particle size distribution and morphology of nanocapsules

In order to study the effects of the emulsifier content on the particle size distribution and morphology of nanocapsules, the emulsifier contents change from 0.1 to 0.9 wt%. In the experiment, the other reaction conditions do not change and only the emulsifier content increase in the reaction system. Figure 1 illustrates the particle size distribution of the nanocapsules at different emulsifier content. The average hydrodynamic diameter and encapsulation efficiency of the resultant samples were summarized in Table 2. The average hydrodynamic diameters of the nanocapsules for 0.1, 0.3, 0.6, and 0.9 wt% of emulsifier content are 250.6, 222.0, 189.7, and 200.5 nm, respectively. As the emulsifier contents increase from 0.1 to 0.6 wt%, the average hydrodynamic diameter of resultant nanocapsule becomes

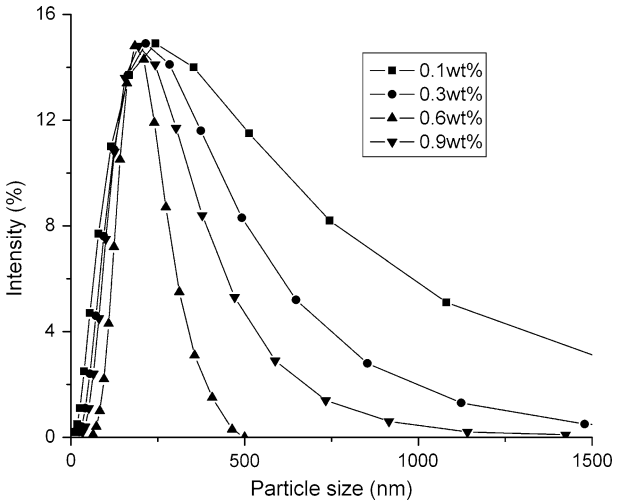

Fig. 1 Particle size distribution of nanocapsules prepared at different emulsifier content

Table 2 The average hydrodynamic diameter and encapsulation efficiency of nanocapsules prepared at different emulsifier content

Percentage weight of emulsifier (wt%)	d (nm)	ϕ (wt%)
0.1	250.6	74.2
0.3	222.0	90.0
0.6	189.7	95.0
0.9	200.5	87.2

smaller and size distribution becomes narrower. During the emulsification process, the emulsifier can decrease the interfacial tension of the system, which the organic phase is easily dispersed into finer droplets. Moreover, the emulsifier can enwrap the surface of dispersed droplets to prevent dispersed droplets from coalescing [18]. And during the emulsion polymerization process, the emulsifier molecules form emulsifier micelles containing core material and wall-forming materials. Polymerization was initiated to form nanocapsules when the water-soluble initiating radical moved to the surface of core material [19]. As a result, the average hydrodynamic diameter of resultant nanocapsule becomes smaller and size distribution becomes narrower with an appropriate increase in emulsifier content. As the emulsifier content increase from 0.6 to 0.9 wt%, the average hydrodynamic diameter of resultant nanocapsule becomes bigger and size distribution becomes broader. The reason may be that excessive emulsifier micelles contain excessive monomers. Therefore, excessive monomers can be reacted rapidly on the surface of the cores to cause coalescence among the particles. The changing of the encapsulation efficiency also confirmed the above explanation. As showed in Table 2, the encapsulation efficiency of the nanocapsules for 0.1, 0.3, 0.6, and 0.9 wt% of emulsifier content is 74.2, 90.0, 95.0, and 87.2 wt%, respectively, in which the encapsulation efficiency is the lowest at emulsifier content being 0.1 wt%. This indicates that, for one thing, the inadequate emulsifier cannot provide dispersion stabilization of droplets to result in coalescing among particles, and for another the low dosage of the emulsifier cannot form enough of an emulsifier micelle containing core material and wall-forming materials. As a result, these cause low encapsulation efficiency.

Figure 2 shows the scanning electron microphotographs of the nanocapsules prepared at different emulsifier content. The SEM image of the emulsifier content of 0.1 wt% was shown in Fig. 2a. Such particles exhibited an irregular shape with evidence of particle aggregation. This was probably due to the poor spatial stabilization resulting from the low emulsifier content. The low dosage of the emulsifier could not provide enough of a spatial barrier among nano-particles with the high surface energy, leading to the particle aggregation. Figure 2b, c showed the image of the nanocapsules prepared with the emulsifier content being 0.3 and 0.6 wt%. The nanocapsules revealed smooth surface and spherical shape and good dispersibility. Figure 3d showed the image of the nanocapsules prepared with the emulsifier content being 0.9 wt%. A rough surface and the coagulation among the particles had been observed. The results of scanning electron photographs were basically consistent with those of the particle distribution measurement.

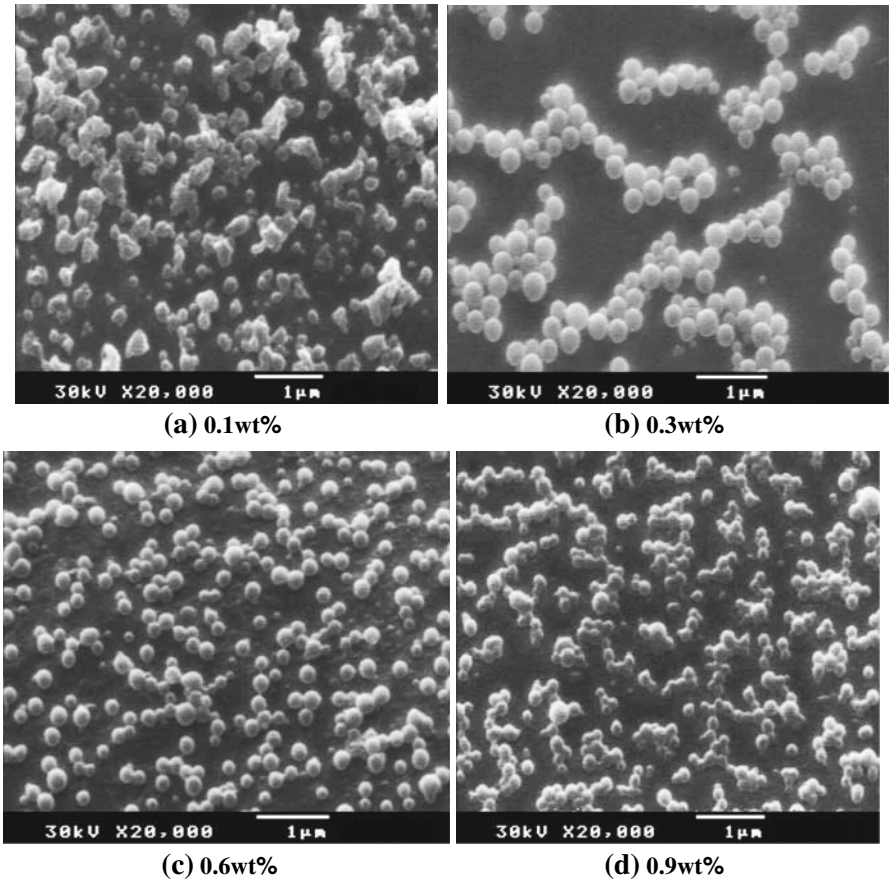

Fig. 2 SEM photographs of nanocapsules prepared at different emulsifier content

Structure of nanocapsules

FTIR Spectroscopy results for the samples are shown in Fig. 3. Figure 3a corresponds to No.3 leucocompound-containing nanocapsules, and Fig. 3b, c to leucocompound and the No.3 shells that were prepared in the same way as the hybrid systems without the addition of leucocompound, respectively. In the spectrum of Fig. 1a, b, N–H stretching at 3,350 cm^{-1}, =C–H stretching in the phenyl ring at 3,040 cm^{-1}, C=C stretching and =C–H out-plane rocking vibration in the phenyl ring at 1,550 and 1,520 cm^{-1}, and 750 and 690 cm^{-1} are observed, indicating that leucocompound is encapsulated in the nanocapsules [20]. In addition, as shown in the spectrum of Fig. 3a, c, the peaks at 1,390 and 1,440 cm^{-1} are attributed to the $–CH_3$ vibration and $CH_3–O$ vibration of MMA, respectively. The peak with wavenumber of 1,640 cm^{-1} corresponds to the amide bond stretching of UHBP [16]. The results confirm that the shells of the nanocapsules are composed of MMA and UHBP as expected.

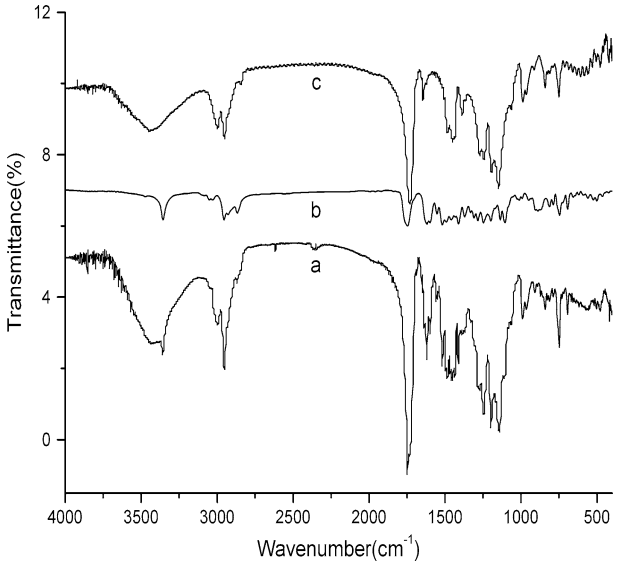

Fig. 3 FTIR spectra of **a** leucocompound-containing nanocapsules, **b** leucocompound and **c** the shells made from MMA/UHBP

Glass transition temperature analysis

The DSC thermograms of No.3 leucocompound-containing nanocapsules and the No.3 shells that were prepared in the same way as the hybrid systems without the addition of leucocompound are depicted in Fig. 4, where the glass-transition temperature (T_g) of the nanocapsules and shells is 117.9 and 128.2 °C, respectively. Evidently, the T_g of the leucocompound-containing nanocapsules is lower than that of the shells. This is due to a plasticization effect of core materials. The core molecule is much smaller than shell polymer molecule, which would increase the movement of polymer segment and result into a decreased T_g. The T_g would have an effect on the heat-sensitive color-developing property of the resultant nanocapsules [1].

In order to investigate the influence of the crosslinking density on T_g of nanocapsules, the T_gs of systems prepared with pure (non-crosslinked) PMMA and with various amounts of crosslinker are evaluated. In the experiment, the particles are prepared without the addition of leucocompound to avoid the effect of the leucocompound on T_g of nanocapsules. Figure 5 shows DSC thermograms of the nanocapsules of pure PMMA and various amounts of crosslinker, respectively. The T_gs of the nanocapsules for pure PMMA and 2.0, 4.0, 6.0, and 10.0 wt% of crosslinker content are 112.2, 121.1, 125.4, 128.2, and 126.2 °C, respectively. The T_g of the nanocapsules becomes higher with the increase in crosslinker content from 0 to 6.0 wt%. This is due to crosslinking density effect. However, The T_g of the nanocapsules decreases with crosslinker content being 10.0 wt%. This may be explained by that excessive macromolecule crosslinker plays a soft-segment role [21].

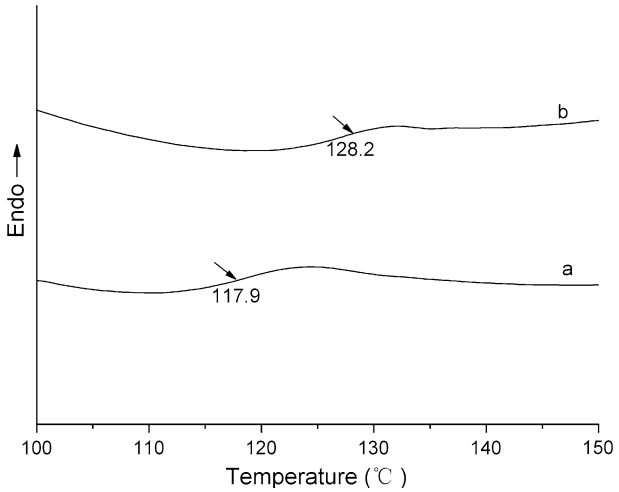

Fig. 4 DSC thermograms of **a** leucocompound-containing nanocapsules and **b** the shells made from MMA/UHBP

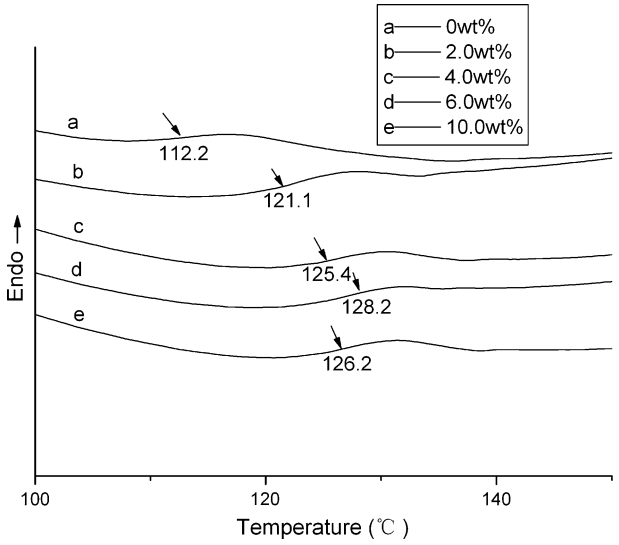

Fig. 5 DSC thermograms of nanocapsules prepared at different amounts of crosslinker

Thermal stability of nanocapsules

Figure 6 shows the TG curves of leucocompound, No.3 leucocompound-containing nanocapsules and the No.3 shells that were prepared in the same way as the hybrid systems without the addition of leucocompound. As shown in Fig. 6 and Table 3, the onset temperatures of the thermal decomposition process for the leucocompound,

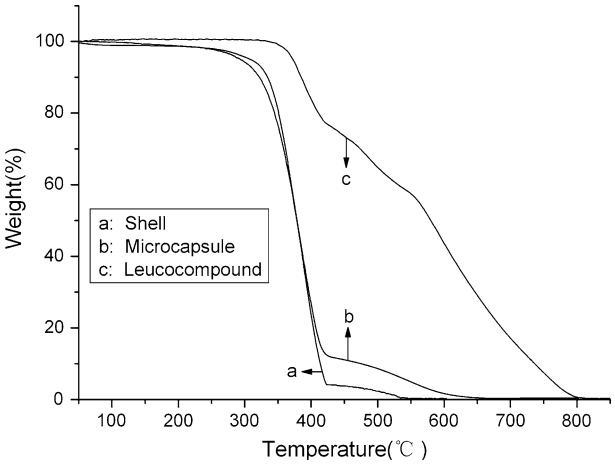

Fig. 6 TG curves of leucocompound, leucocompound-containing nanocapsules and the shells made from MMA/UHBP

Table 3 Pyrolytic characteristics of leucocompound, leucocompound-containing nanocapsules and the shells made from MMA/UHBP

Material	First pyrolytic stage		Second pyrolytic stage	
	$T^{a}_{1,\ onset}$ (°C)	$T^{b}_{1,\ end}$ (°C)	$T^{a}_{2,\ onset}$ (°C)	$T^{b}_{2,\ end}$ (°C)
Leucocompound	360	422	549	796
Nanocapsule	308	426	426	643
Shell	293	426	426	536

[a] $T_{1,\ onset}$, $T_{2,\ onset}$: onset temperatures of the first and second pyrolytic stages, respectively

[b] $T_{1,\ end}$, $T_{2,\ end}$: end temperatures of the first and second pyrolytic stages, respectively

leucocompound-containing nanocapsules, and the shells are 360, 308, and 293 °C. The onset temperature of the thermal decomposition process for the leucocompound-containing nanocapsules is slightly higher than that for the shells. This result seems to be caused by the thermally stable leucocompound itself. In addition, the onset temperatures of the thermal decomposition process for the leucocompound, leucocompound-containing nanocapsules, and the shells are higher than the T_g of the leucocompound-containing nanocapsules, which is especially fit for the application of the heat sensitive nanocapsules.

Heat sensitive color-developing properties

Figure 7 illustrates the heat sensitive color-developing density of the resultant nanocapsules at different emulsifier content, in which the values of density have no change below 95 °C at the emulsifier content being 0.3 and 0.6 wt%, confirming that the walls of resultant nanocapsules are compact. And when the nanocapsules prepared at both 0.3 and 0.6 wt% were heated above 95 °C, the color-developing

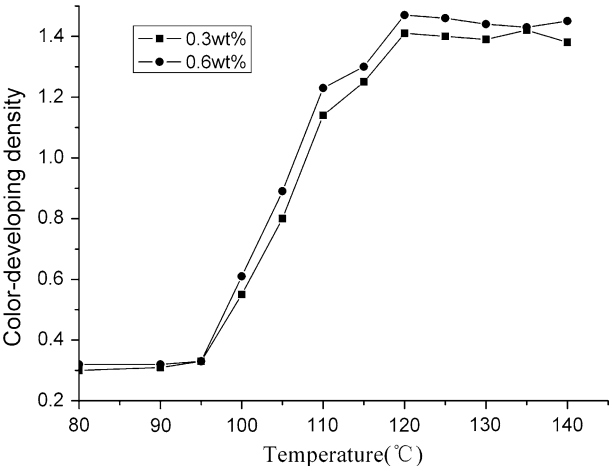

Fig. 7 Heat sensitive color-developing density of nanocapsules prepared at different emulsifier content

density values increased with increasing the temperature. This is due to when the wall of the nanocapsule is heated above its glass transition temperature (112.1–123.8 °C, see Fig. 4a), the transmittance of the wall material increases and a color-developing component contained in the core and outside of the nanocapsule transmits the wall of the nanocapsule to develop a color. In addition, the color-developing density value from the nanocapsules at the emulsifier content being 0.6 wt% is higher than that from the nanocapsules at the emulsifier content being 0.3 wt% at the same temperature. The reason should be that the average hydrodynamic diameter from the nanocapsules at the emulsifier content being 0.6 wt% is smaller than that from the nanocapsules at the emulsifier content being 0.3 wt%, and smaller particle size nanocapsules would have larger total specific surface area, therefore causing the density to be higher than that of larger particle size nanocapsules at the same temperature. This outcome is consistent with the research of the relation between particle size and sustained release rate by Yamamoto et al. [22]. Furthermore, the encapsulation efficiency of the nanocapsules at the emulsifier content being 0.6 wt% is higher than that of the nanocapsules at the emulsifier content being 0.3 wt%, leading to higher density with the emulsifier content being 0.6 wt% at the same temperature.

Conclusions

The crosslinked poly(methylmethacrylate) heat sensitive color-developing nanocapsules have been synthesized by emulsion polymerization, in which leucocompound is used as core material and methyl methacrylate and unsaturated hyperbranched poly(amide-ester) as wall-forming materials. The FTIR analysis of leucocompound-containing nanocapsules demonstrates that the leucocompound is successfully encapsulated in the crosslinked PMMA matrix. TGA results show that the resultant nanocapsules had good thermal stabilities. The DSC analysis of the resultant

nanocapsules indicates that the glass transition temperature of the nanocapsules was 117.9 °C. The resultant nanocapsules have narrower particle size distribution, smoother surface and higher heat sensitive color-developing density with the percentage weight of emulsifier being 0.6 wt%.

Acknowledgments This work was supported by National Natural Science Foundation (20574016), and the Natural Science Foundation (B2004000093) of Hebei Province.

References

1. Kamikawa H, Shizuoka K (2003) US Patent Office 20,030,191,022 A1
2. Sawada K, Urakawa H (2005) Dyes Pigments 65:45–49
3. Arshady R (1990) Polym Eng Sci 30:915
4. Arshady R (1993) Polym Eng Sci 33:865
5. Vinetsky Y, Magdassi S (1999) Microencapsulations in cosmetics, novel cosmetic delivery systems. Marcel Dekker, Inc., New York, p 295
6. Ding SX, Min ZR, Ming QZ (2007) Polymer 48:4765
7. Damge C, Aprahamian M, Balboni G et al (1987) Int J Pharm 36:121
8. Wang JP, Zhao XP, Guo HL (2004) Langmuir 20:10845
9. Andrew L, Brian V (1998) J Colloid Interface Sci 208:49
10. Ishizu K, Takahashi D, Takeda H (2000) Polymer 41:6081
11. Gao C, Yan DY (2004) J Prog Polym Sci 29:183
12. Parker D, Feast WJ (2001) Macromolecules 34:5792
13. Thomasson D, Boisson F, Girard-Reydet E, Me′chin F (2006) React Funct Polym 66:1462
14. Uhrich KE, Hawker CJ, Frechet JMJ (1992) Macromolecules 25:4583
15. Hong K, Nakayama K, Park S (2002) J Eur Polym 38:305
16. Li CZ, Wang SJ, Ba XW (2006) J Hebei Univ 26:270
17. Chang CP, Chang JC, Ichikawa K, Dobashi T (2005) Colloid Surf B 44:187
18. Chao DY (1993) J Appl Polym Sci 47:645
19. Liang ZQ (1999) Technology and application of microcapsule. China Light Industry Press, Beijing, p 135
20. Hong K, Park S (2000) Polym Test 19:975
21. Wang XX, Lai GQ, Jiang ZG, Zhang YF (2006) J Eur Polym 42:286
22. Yamamoto T, Dobashi T, Kimura M, Chang CP (2002) Colloid Surf B 25:305